Scripta Materialia 126 (2017) 33–36

Contents lists available at ScienceDirect

Scripta Materialia

journal homepage: www.elsevier.com/locate/scriptamat

Regular Article

A new type of WC–Co–Ni–Al cemented carbide: Grain size and morphology of γ'-strengthened composite binder phase

Jianzhan Long [a,b], Weibin Zhang [a], Yaru Wang [a,c], Yong Du [a,*], Zhongjian Zhang [b], Bizhi Lu [b], Kaiming Cheng [a,d], Yingbiao Peng [e]

[a] State Key Laboratory of Powder Metallurgy, Central South University, Changsha, Hunan 410083, PR China
[b] State Key Laboratory of Cemented Carbide, Zhuzhou, Hunan 412000, PR China
[c] School of Materials Science and Engineering, Shijiazhuang Tiedao University, Shijiazhuang, Hebei 050043, PR China
[d] Shandong Key Laboratory of High Strength Lightweight Metallic Materials, Advanced Materials Institute, Shandong Academy of Sciences, Jinan, Shandong 250014, PR China
[e] School of Metallurgical Engineering, Hunan University of Technology, Zhuzhou 412007, PR China

ARTICLE INFO

Article history:
Received 25 June 2016
Received in revised form 3 August 2016
Accepted 8 August 2016
Available online xxxx

Keywords:
Cermets
Thermodynamics
Grain boundaries
Electron backscatter diffraction (EBSD)
Driving force for nucleation

ABSTRACT

In contrast to the much larger grain size of the binder phase in traditional WC–Co cemented carbide, we have achieved a significantly reduced grain size of the γ'-Ni_3Al strengthened composite binder phase in WC–Co–Ni–Al cemented carbide. Based on thermodynamic calculations, decisive experiments and microstructure characterizations, the formation mechanism for grain size of binder phase in WC–Co–Ni–Al cemented carbide has been clarified, and the related boundary morphology and performance characteristics are discussed.

WC–Co cemented carbides are widely used in many industrial applications due to their good combination of high hardness and good fracture toughness, such as in cutting, milling, turning and rock drilling [1,2]. It is realized that the mechanical properties of cemented carbides are closely related to their microstructure, especially the phase composition, phase distribution and grain size [3]. It has been shown that the grain size and morphology of WC have a great impact on the properties of traditional WC–Co cemented carbides [4]. To further improve mechanical properties of the WC–Co cemented carbides, strengthening the Co binder phase has been the subject of many investigations [1,5–8]. In the field of cobalt-based superalloys, the discovery of the ordered fcc_$L1_2$ γ'-$Co_3(Al,W)$ [9] in the Al–Co–W system has initiated extensive investigations about $L1_2$-strengthened cobalt-based superalloys [10]. Novel γ (disordered fcc_Al) + γ' Co-based superalloys have demonstrated a better high temperature strength than the conventional Co-based alloys [11,12]. Meanwhile, the stability of γ' phase is greatly increased through Ni substitution for Co [13]. Therefore, it offers new possibilities for development of novel WC–Co–Ni–Al cemented carbides, that possess both high-temperature strength and environmental corrosion resistance [5,6]. It is expected that such WC–Co–Ni–Al cemented carbides are of potential industry application in the field of high temperature domains.

Herein we design different Co–Ni–Al compositions of binder phase that are responsive to the grain size and morphology of γ'-strengthened composite binder phase. By an integrated approach of thermodynamic calculations and calculation-guided experiments, the main factors affecting the grain size and morphology of γ'-strengthened composite binder phase could be revealed. With the reduced grain size of Co–Ni–Al binder phase and γ' phase precipitation, both the hardness of binder and the coercivity of WC–Co–Ni–Al materials increase dramatically. The calculated nucleation driving force, interfacial energy and related boundary morphology of the Co–Ni–Al binder phase are discussed in detail.

In order to make the difference of binder grain size more apparent, we chose to use a WC–50 wt.% (Co–Ni–Al) alloy with the same carbon content and coarse crystal WC grains (9 μm) as the starting materials. Prior to the experiment, the driving force for the nucleation of the γ-binder precipitate from liquid phase at 1250 °C was calculated in order to select the optimal alloy composition, as shown in Fig. 1(a). It is shown that the calculated driving force for the precipitation from liquid increases with increasing Ni_3Al content. Thus the composition of the Co–Ni–Al binder phase is important for controlling the driving force for the nucleation of binder phase during solidification, which in turn affects grain size and morphology of the binder phase. Generally, the

---

* Corresponding author.
E-mail address: yong-du@csu.edu.cn (Y. Du).

http://dx.doi.org/10.1016/j.scriptamat.2016.08.007
1359-6462/

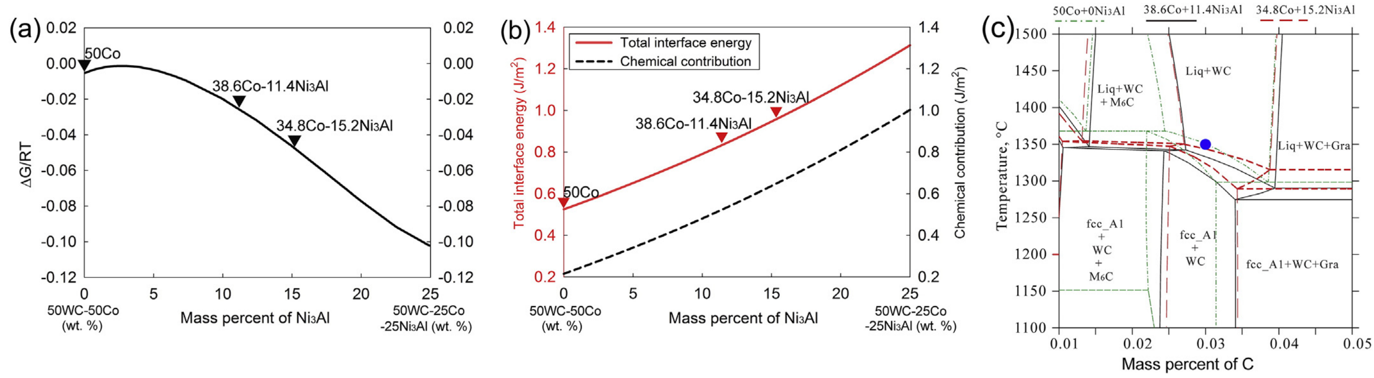

Fig. 1. (a) calculated driving force of the precipitation of the γ-binder phase from liquid in WC–50(Co–Ni–Al) with different binder composites at 1250 °C; (b) the solid-liquid interfacial energy in WC–50(Co–Ni–Al) with different Ni_3Al contents; (c) calculated phase equilibria in WC–50(Co–Ni–Al).

Co-binder phase nucleates against a WC grain due to its energetically favorable boundaries [14], and its microstructure depends largely on the related interfacial energy between WC and liquid Co binder phase [3]. According to the thermodynamic model by Warren [15], the solid-liquid interfacial energy can be estimated by considering the chemical contribution and the structure contribution. The structure contribution remains constant (0.31 J/m^2) since it depends on the melting point of WC grain [15], while the chemical contribution of binder metal, which changes with Co–Ni–Al chemical compositions, can be calculated by using Thermo-Calc software [16] applied to the thermodynamic database developed by Peng et al. [17]. As indicated in Fig. 1(b), the short dashed line represents the chemical contribution of the WC–50(Co–Ni–Al) interfacial energy at various Ni_3Al contents. It can be seen that the chemical contribution shows a minimum value of 0.215 J/m^2 at the composition of WC–50Co, and increases with increasing Ni_3Al content until 1.003 J/m^2 at the composition of WC–25Co–25Ni_3Al.

Based on the above calculations, three WC–50(Co–Ni–Al) alloys containing 0, 11.4 and 15.2 wt.% Ni_3Al were synthesized in the present work. Thermodynamic calculations for three WC–50(Co–Ni–Al) alloys were performed based on our thermodynamic database CSUTDCC1 [17,18] in order to select the appropriate carbon content and sintering temperature, as shown in Fig. 1(c). The computed γ + WC phase region shows some difference for carbon content ranges and sintering temperature with different Ni_3Al contents. The WC + Ni_3Al pre-alloyed powders were prepared in a vacuum furnace with a vacuum degree of 1 Pa by reaction synthesis of pure carbonyl Ni, analytical reagent Al and WC powders (9 µm) in the temperature range of 1100–1200 °C using the processing conditions previously described by Long et al. [19]. These alloys were then prepared from a powder mixture of WC, Co powders and WC + Ni_3Al pre-alloyed powders through a powder metallurgical technique. The mixed powders were milled for 24 h in alcohol medium with ball to powder weight ratio of 3:1. Based on the above calculations, the carbon content of samples used in the present work was controlled to be 3 wt.% to avoid the formation of η (M_6C) or graphite phases by adjusting W or C content [2], and the samples were sintered at 1350 °C for 1 h in vacuum, as shown in blue circle in Fig. 1(c).

The microstructure and orientation of the binder phase in the as-sintered samples were investigated using electron backscattered diffraction (EBSD). The EBSD analysis was operated at 20 kV in an FEI Helios Nanolab 600i instrument with the HKL system and the HKL Channel 5 software. A step size of 100 nm was used. In addition, the local microstructure of the binder phase in the as-sintered samples was examined by field emission scanning electron microscopy (FE-SEM, JEOL JSM 6701F) and transmission electron microscopy (TEM, FEI Titan G2 60-300). As shown in Fig. 1(c), there are γ and WC phases from 1100 °C to the solidus temperature of 1310–1327 °C for these prepared alloys. In order to analyze the effect of the grain size of binder phase on the mechanical property and avoid the effect of γ′ precipitation at lower temperatures (~700 °C), the solid solution treatment was carried out at 1250 °C for the as-sintered samples. Fast cooling from 1250 °C to room temperature was performed via quenching with a cooling rate of about 100 °C/min. After the treatment, the coercivity (*Hc*) was determined using an YSK-I tester. A microhardness tester was used to determine the Vickers hardness (HV) of the binder using a load of 10 g.

Table 1 lists the measured grain size of the binder phase in the as-sintered samples along with the literature data [14,20–23]. Using X-ray diffraction, many previous investigations [20,21,23] have shown that the binder forms a skeleton of its own, in which the lattice orientation is constant over distances as large as 50–100 µm. Thus the effective grain size of the binder is much larger than that of the carbide. Although binder grains are interpenetrated by WC grains, they can be delimited according to their orientation using the EBSD method. Recently, some works [14,22] have been published on the grain size and morphology of Co binder phase using EBSD. Mingard et al. [22] also demonstrated that the binder phase is shown to form very large regions of a single-crystallographic orientation up to 50 times greater than the mean size of the WC grains.

According to the present work, the grain size of the Co-binder phase is above 200 µm for the WC–50Co alloy, which is larger than 100–200 µm observed in the traditional WC–Co-cemented carbide [22] due to the higher Co-binder content and the coarser WC grain size used in the present work. The presently observed large grain size is consistent with the previous conclusions [14] that fine WC grain size and a low content of the binder phase lead to small grain size of binder phase, owing to more nucleation particles for binder nucleating. It is also expected that the large grain size of the Co-binder phase is associated with the low driving force for nucleation of −0.006 at 1250 °C during solidification and the low solid-liquid interfacial energy of 0.525 J/m^2. Fig. 2 presents the EBSD maps of WC–38.6Co–11.4Ni_3Al and WC–34.8Co–15.2Ni_3Al with the orientation of the binder phase shown in a color inverse pole figure (IPF). In the case of WC–38.6Co–11.4Ni_3Al alloy, a grain size of about 100 µm for the binder phase is obtained, as

Table 1
Grain sizes of binder phase and WC (equivalent circle diameter).

Material	Detection method	WC grain size (µm)	Binder phase grain size (µm)
WC–10Co,WC–20Co [20]	XRD	–	100–700
WC–6Co, WC–15Co [21]	XRD	5.0	50–100
WC–(6–10)Co [14]	EBSD	0.4–0.8	26–49
WC–6Co [22]	EBSD	4.1	100–200
WC–10Co [22]	EBSD	1.0	100
WC–11Co [22]	EBSD	5.0	100–200
WC–50Co (this work)	EBSD	9–10	≥200
WC–38.6Co–11.4Ni3Al (this work)	EBSD	9–10	~100
WC–34.8Co–15.2Ni3Al (this work)	EBSD	9–10	~20